Hindawi Publishing Corporation
International Journal of Photoenergy
Volume 2012, Article ID 367072, 8 pages
doi:10.1155/2012/367072

Research Article

The Photocatalytic Inactivation Effect of Fe-Doped TiO_2 Nanocomposites on Leukemic HL60 Cells-Based Photodynamic Therapy

Kangqiang Huang,[1] Li Chen,[2] Meixiang Liao,[3] and Jianwen Xiong[1]

[1] *Laboratory of Quantum Information Technology, School of Physics and Telecommunication Engineering, South China Normal University, Guangzhou 510006, China*
[2] *Department of Physics and Optoelectronic Engineering, Guangdong University of Technology, Guangzhou 510006, China*
[3] *School of Physics and Engineering, Sun Yat-sen University, Guangzhou 510275, China*

Correspondence should be addressed to Jianwen Xiong, jwxiong@scnu.edu.cn

Received 7 October 2011; Revised 6 December 2011; Accepted 6 December 2011

Academic Editor: Jiaguo Yu

The Fe-doped TiO_2 nanocomposites synthesized by a deposition-precipitation method were characterized by X-ray diffraction (XRD), transmission electron microscope (TEM), X-ray photoelectron spectroscopy (XPS), and UV-vis adsorption spectra and then were taken as a new "photosensitizer" for photodynamic therapy (PDT). The photocatalytic inactivation of Fe-doped TiO_2 on Leukemic HL60 cells was investigated using PDT reaction chamber based on LED light source, and the viability of HL60 cells was examined by Cell Counting Kit-8 (CCK-8) assay. The experimental results showed that the growth of leukemic HL60 cells was significantly inhibited by adding TiO_2 nanoparticles, and the inactivation efficiency could be effectively enhanced by the surface modification of TiO_2 nanoparticles with Fe doping. Furthermore, the optimized conditions were achieved at 5 wt% Fe/TiO_2 at a final concentration of 200 μg/mL, in which up to 82.5% PDT efficiency for the HL60 cells can be obtained under the irradiation of 403 nm light (the power density is 5 mW/cm^2) within 60 minutes.

1. Introduction

Photodynamic therapy (PDT) is a new technique for cancer treatment. It takes advantage of the selective accumulation of photosensitizers, which accumulate in tumor tissues and produce singlet oxygen to inactivate the tumor cells through series of the photochemical reactions or photobiological reactions at a specific light wavelength within the absorption spectra of the photosensitizer, to achieve local treatment purposes [1]. In PDT, light, oxygen, and photosensitizer are combined to produce a selective therapeutic effect in the target tissue [2, 3]. Among these three agents, photosensitizer, as the energy carrier and the interaction bridge, is playing an important role in tumor treatment [1, 4]. However, tumors in human body with varying degrees of depth the application of traditional photosensitizers is restricted because of their inherent properties. Therefore, seeking for a high-performance photosensitizer and improving the existing properties of photosensitizer have become the main focus of PDT study.

Compared to other semiconductor oxides, TiO_2 has been widely used and proved to be an important potential photosensitizer because of their unique physical and biological properties [5–7], such as photostable, inexpensive, nontoxic properties, and it has high oxidative power, no secondary pollution. Moreover, with the rapidly development of nanotechnology, nanoparticles have shown a wide range of potential applications in biological and biomedical fields [8–11]. TiO_2 nanoparticles as an anticancer drug or used for energy transfer material to improve the traditional photodynamic effect have been noticed [12–15]. Nevertheless, the electron-hole pairs of TiO_2 can be formed only under ultraviolet light. Additionally, the photogenerated holes are easy to recombine with the photoinduced electrons, which

greatly reduce the photocatalytic inactivation efficiency of TiO_2 nanoparticles and hinder its practical applications [16–19]. Fortunately, it has been demonstrated that the photocatalytic efficiency and the visible light absorption of TiO_2 can be effectively improved by the method of transition metal doping [20–23].

In this paper, nanoparticles of TiO_2 and Fe-doped TiO_2 were used as a photosensitizer to kill cancer cells. Up to our knowledge, there still no previous report on the study of photocatalytic inactivation effects of Fe/TiO_2 on HL60 cells. Our experimental results show that the photocatalytic inactivation efficiency on human HL60 cancer cells could be greatly enhanced by the Fe modification of TiO_2 nanoparticles, which have not only significantly improved the selective inactivation of tumor cells *in vitro* and accurate PDT dosimetry, but also have potential clinical applications when TiO_2 nanoparticles are used as a photosensitizer or energy transferor in photodynamic therapy.

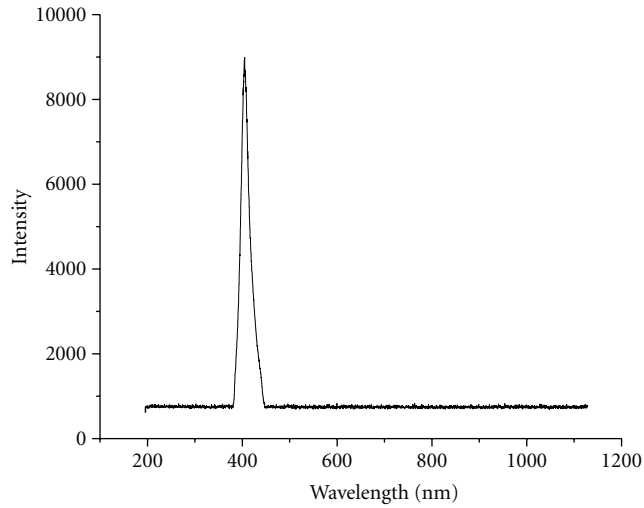

Figure 1: The emission spectra of the blue LEDs.

2. Materials and Methods

2.1. Chemicals and Apparatus. HL60 cells were kindly provided by the Department of Medicine of Sun Yat-sen University in China. The TiO_2 nanoparticles, Fe/TiO_2 (2%) and Fe/TiO_2 (5%) nanocomposites, 5-aminolevulinic acid (ALA) and phosphate buffered saline (PBS) were purchased from Sigma (USA). The Cell Counting Kit-8 (CCK-8) was purchased from Dojindo (Japan). RPMI medium 1640 and foetal calf serum (FCS) were obtained from Gibco BRL (USA). All chemicals used were of the highest purity commercially available. The stock solutions of the compounds were prepared in serum-free medium immediately before using in experiments.

These apparatus, including D8 Focus X-ray diffraction (XRD) (Bruker, Germany), AXIS Ultra X-ray photoelectron spectroscopy (XPS) (Kratos, UK), U-3010 UV-visible spectrophotometer (Hitachi, Japan), JEM-2100HR transmission electron microscope (TEM, Japan), HH.CP-TW80 CO_2 incubator, DG5031 ELISA reader, XDS-1A inverted microscope, PDT reaction chamber, 96-well plates, cell count board, and so on were used in this research.

2.2. Light Source. To reach a high efficiency of PDT, An in-house built lamp with many high-power light-emitting diodes (LEDs), emitting light in the visible-light region 400–410 nm and with a peak at 403 nm, was taken as light sources in the experiments. The fluence rate at the position of the sample was 5 mW/cm^2 as measured with a photodiode. As shown in Figure 1, the blue LEDs can better meet the needs of PDT experiments.

2.3. Preparation of TiO_2 Nanoparticles and Fe-Doped TiO_2 Nanocomposites Solutions. The pure TiO_2 nanoparticles, 2 wt% Fe/TiO_2 and 5 wt% Fe/TiO_2 nanocomposites, were synthesized using the deposition-precipitation method. Firstly, $Ti(SO_4)_2$ (6 g), neopelex (DBS, 0.18 g), $CO(NH_2)_2$ (32 g), definite volumes of doubly distilled water (250 mL), absolute ethyl alcohol (0.25 mL), and 98% H_2SO_4 were mixed with appropriate amount of $Fe_2(SO_4)_3$ (0 g, 0.1 g, 0.5 g resp.) to make up the reaction liquid, which then would be treated in water bath at 80°C under vigorous stirring for 2 to 3 hours at pH 8. Afterwards, the reactant was transferred from the water bath to be deposited for 24 h. The third process was the washing and filtering, SO_4^{2-} and DBS were removed by washing with deionized water. $BaCl_2$ solution was employed to check whether SO_4^{2-} exists. The formatting of $BaSO_4$ white sediment indicated more washing was needed. The resulting precipitates were washed again with ethyl before dehydration, drying in the dry-box for 3 h. Finally, The Fe-doped TiO_2 was obtained after calcined at 400°C for 30 min and grinded for 15 min.

The prepared nanoparticles were encapsulated in three bottles, respectively. Subsequently, they were placed in YX-280B-type pressure steam sterilizer with a high temperature and high pressure (120°C, 1.5 atm) to sterilize for 30 minutes. Finally, an appropriate amount of culture medium was added to fully dissolve the nanoparticles. All solutions were filtered through a 0.22 μm membrane filter and stored in the dark at 4°C before taken into the experiments.

2.4. Cell Culture. Human leukemia HL60 cells were cultured in RPMI 1640 medium supplemented with 10% fetal bovine serum (FBS) in a humidified incubator with 5% CO_2 at 37°C until confluent. All experiments were performed using cells during the logarithmic growth phase. The cell concentration was measured using a cell count board and the cell density was adjusted to the required final concentration.

2.5. Cell Viability Assay. There are many ways to check the cell viability. The method of CCK-8 (Cell Counting Kit-8), which is much simpler, more sensitive, and reproducible than the traditional method of MTT [24], was used to detect the activation of cell during the experiment. CCK-8 assay based on the ability of a mitochondrial dehydrogenase enzyme from viable cells contains WST-8, which can be reduced to

a highly water-soluble yellow-colored formazan dye by dehydrogenase in the presence of an electron carrier (1-methoxy PMS). The number of surviving cells is directly proportional to the level of the formazan product created. The amount of formazan dye can be reflected by the absorbance at 450 nm. Therefore, the characteristic of CCK-8 can be used directly for cell proliferation and toxicity analysis.

2.6. Experimental Design. Firstly, 96-well plates were divided into several parts according to experimental needs (including the control groups and zero groups). Three repeated wells were set under the same experimental conditions. Secondly, HL60 cells in logarithmic growth phase were seeded in 96-well plates, afterwards the prepared solutions of TiO_2, Fe/TiO_2 (2%), Fe/TiO_2 (5%) at various concentrations were added in the appropriate samples respectively, and each well was infused with an appropriate volume of cell culture medium to ensure that the final volume was 200 μL, while the zero pores contain only 200 μL of culture medium. Thirdly, light exposure was carried out immediately after 4 h incubation (The average fluence rate used was 5 mW/cm^2, the irradiation dose was 18 J/cm^2). After that, 20 μL of solution was added to each well and incubated for other 4 hours. Finally, the OD values of the samples were detected by the ELISA reader based on dual-wavelength method (the test wavelength at 450 nm and reference wavelength at 630 nm). Three parallel tests were performed for each sample to ensure accuracy.

2.7. Statistical Analysis. Data are presented as means ± S.D. (standard deviation) from at least three independent experiments. Statistical analysis was then performed using the statistical software SPSS11.5, Values of $P < 0.05$ were considered statistically significant.

3. Results and Discussion

3.1. Characterization of Fe-TiO_2 Nanocomposites

3.1.1. X-Ray Diffraction. The crystallite size is calculated by the Scherrer formula [25]:

$$D = \frac{K\lambda}{\beta \cos\theta}, \quad (1)$$

where D is the crystalline size, λ is the X-ray wavelength (0.1541 nm), K is the constant usually taken as 0.89, θ is the Bragg's angle $2\theta = 25.3^\circ$ for anatase phase titania, and β is the pure full width of the diffraction line at half of the maximum intensity. According to the above formula, it is estimated that the average particle sizes are 20.2 nm, 19.8 nm, 17.2 nm for pure TiO_2, 2 wt% Fe-doped TiO_2, and 5 wt% Fe-doped TiO_2, respectively. Apparently, the incorporation of Fe into TiO_2 could effectively inhibit the crystal grain growth of TiO_2, leading to smaller particle.

XRD was also used to further examine the average crystalline properties of the Fe-doped TiO_2. As shown in Figure 2, the XRD diffraction peaks of the synthesized Fe-doped samples around 2θ of 25.26°, 37.73°, 48.28°, 54.36°, 56.43°, 62.17°, which could be indexed to the characteristic peaks (1 0 1), (0 0 4), (2 0 0), (1 0 5), (2 1 1), and (2 0 4) of anatase TiO_2. Thus, the Fe-doped TiO_2 nanocomposites obtained by the deposition-precipitation method have primarily the anatase phase. Furthermore, it is demonstrated that the diffraction peaks of Fe-doped TiO_2 gradually shift towards smaller angle with the increase of Fe-doping concentration compared with that of pure TiO_2, indicating that the lattices of TiO_2 have been expanded by the Fe-doping, which make it possible for Fe^{3+} to diffuse into the TiO_2 lattices to replace Ti^{4+}. Additionally, there is no indication of a peak corresponding to iron oxide (Fe_2O_3) observed, further indicating that Fe^{3+} exists by replacing part of Ti^{4+} in the crystal lattices of TiO_2, which is mainly contributed to the ionic radius of Fe^{3+} (0.064 nm) to be almost equal to that of Ti^{4+} (0.068 nm).

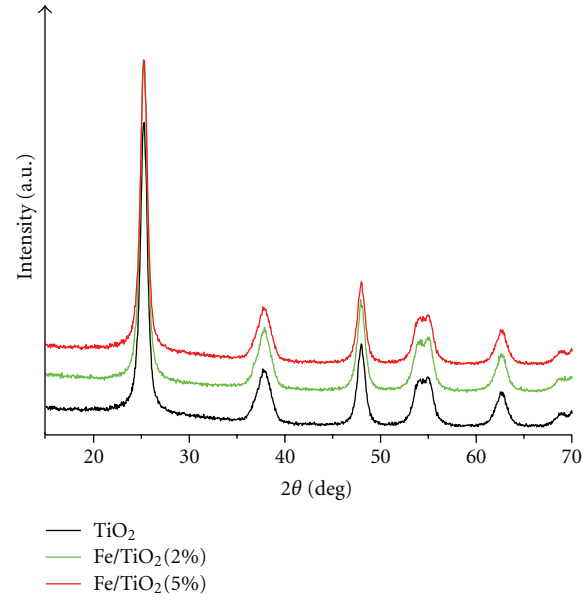

Figure 2: The XRD patterns of TiO_2 nanoparticles and Fe-doped TiO_2 nanocomposites calcined at 400°C.

3.1.2. TEM Studies. The morphology and size of the Fe-doped TiO_2 nanocomposites were studied with a JEM-2100HR transmission electron microscope. As can be seen in Figure 3, TiO_2 particles are spherical or square-shaped with a primary particle size of approximately 18 nm. The measurements are basically consistent with the XRD results.

3.1.3. XPS Analysis. In order to determine whether the successful implementation of the Fe doping, the surface of Fe/TiO_2 (5%) nanocomposites calcined at 400°C has been investigated using XPS analysis. As can be observed from Figure 4, the characteristic peak corresponding to Fe_{2p} is located at 710 eV, which reveals that Fe in the doped samples exists mainly in the form of Fe^{3+} [26]. The result is consistent with the results obtained by X-ray diffraction. Additionally, according to the XPS measurements, the concentration of

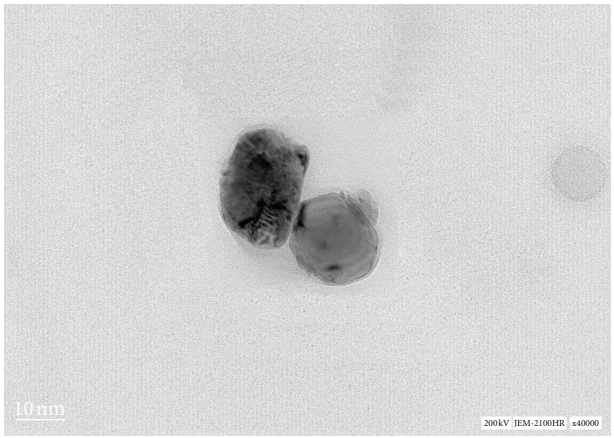

Figure 3: The TEM images of 5 wt% Fe/TiO_2 nanocomposites prepared by deposition-precipitation method.

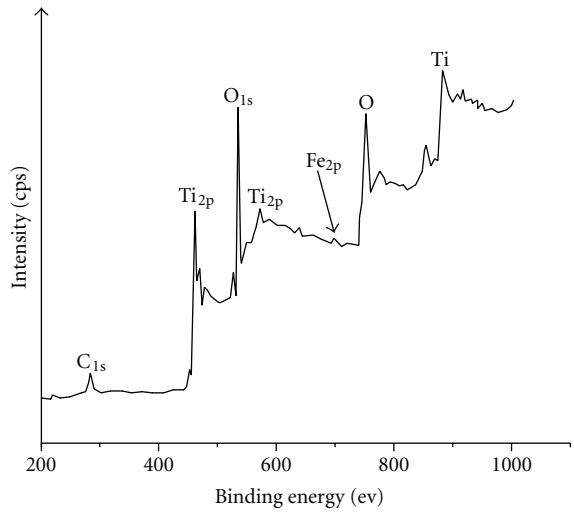

Figure 4: The XPS spectra of Fe/TiO_2 (5%) calcined at 400°C.

Fe over the surface of TiO_2 is 4.68 wt%, which is basically consistent with the theoretical expectation.

3.1.4. UV-Vis Spectroscopy. The UV-visible absorption spectra of TiO_2 nanoparticles doped with different amounts of Fe in the visible light region were measured using U-3010 UV-visible spectrometer, as shown in Figure 5.

The UV-Vis absorption spectra show that the absorption edges of Fe-doped TiO_2 nanoparticles are slightly shifted to longer wavelengths "red-shift" with increasing amount of Fe, and the absorption for the doped TiO_2 in the visible light region is significantly enhanced compared with that of pure TiO_2. Additionally, as shown in Figure 5, the starting point of absorption edge of updoped TiO_2 is 393 nm while that for Fe/TiO_2 (2%) is 407 nm and Fe/TiO_2 (5%) is 425 nm, indicating that the visible light absorption of TiO_2 nanoparticles has been effectively enhanced by the surface modification with Fe.

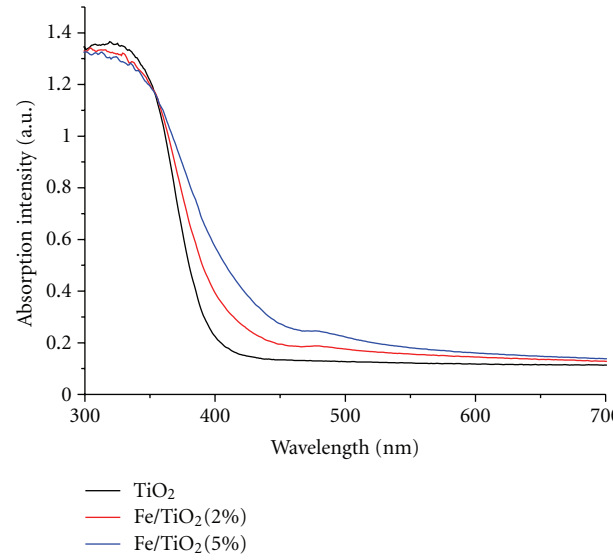

Figure 5: The UV-Vis absorption spectra of TiO_2 with different amounts of Fe doping.

3.2. Effects of Photoexcited TiO_2 with or without Fe Doping on Proliferation of HL60 Cells. HL60 cells in the logarithmic phase at a density of 1×10^5 cells/mL were seeded into 96-well culture plates which had been divided into 4 groups, namely: the control group, the TiO_2 group, the Fe/TiO_2 (2%) group, the Fe/TiO_2 (5%) group, respectively. The final concentration of the groups with nanoparticles was 200 μg/mL. Besides, some culture media were added, respectively, so as to the total volume is 200 μL per well. The optical density values (OD values) of the samples were measured by DG5031 ELISA reader for 6 consecutive days without adding nutrients. The experimental data are presented in Figure 6.

As can be seen from Figure 6, all the HL60 cells showed a low growth rate on the first day indicating they were in the adaptation period. The growth rate for the HL60 cells increased rapidly in the logarithmic phase during the next three days. In this paper, the cells during this period were used in all experiments. On the fifth day, due to nutrient depletion, metabolite accumulation, and environmental changes, the growth rate of cells becomes more and more slow and stabilized downgradually. With the continuous depletion of nutrients and the accumulation of toxic metabolites, the number of viable cells started to decrease from the sixth day.

Figure 6 also demonstrates that the OD values of the experimental groups in the presence of nanoparticles are much lower and with a shorter growth phase than that of the control group under the same conditions. Apparently, TiO_2 nanoparticles or Fe/TiO_2 nanocomposites have a certain degree of inhibitory or toxic effects on the proliferation of HL60 cells. Moreover, the inhibition effects on HL60 cells become more and more obvious with the increasing Fe-doping concentration.

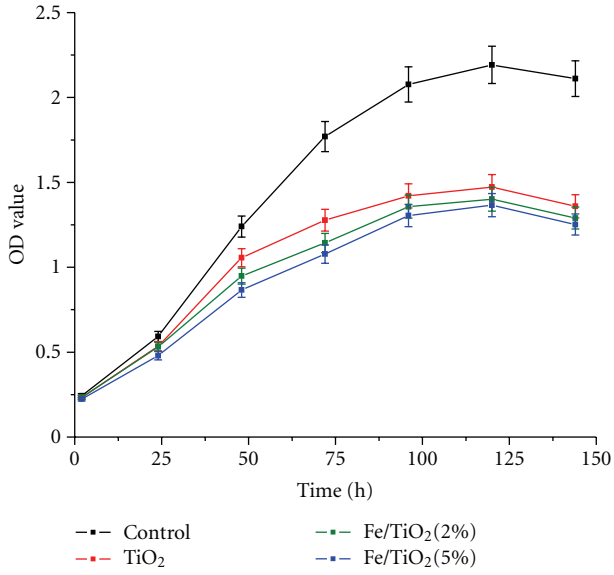

Figure 6: The influence of different nanoparticles on the proliferation of HL60 cells. Data represent the means ± S.D. (standard deviation) from five independent experiments. $^*P < 0.05$ as compared to control (untreated) cells.

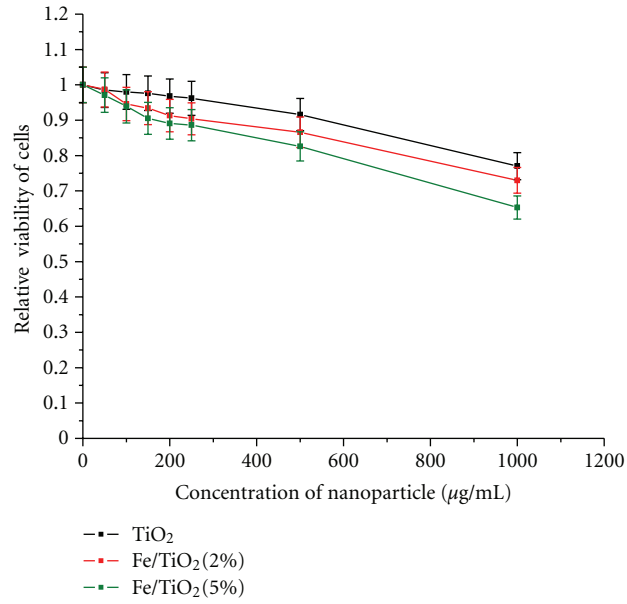

Figure 7: The influence of nanomaterial concentration on the relative viability of HL60 cells. Data are presented as the means ± S.D. from five independent measurements. $^*P$ values are less than 0.05 as compard with untreated control cells.

3.3. Influence of Nanoparticles Concentrations on the Relative Survival of HL60 Cells. It is required for the photosensitive antitumor drugs used in PDT not only to have high photocatalytic inactivation capability under light irradiation, but also to have no toxicity in the dark. Therefore, it is very important to investigate the self-generated toxicity of TiO_2 nanoparticles or Fe/TiO_2 nanocomposites. The toxicity of TiO_2 or Fe/TiO_2 was measured by exposing HL60 cells in the medium containing various concentrations of TiO_2 or Fe/TiO_2 (0 μg/mL, 50 μg/mL, 100 μgL/mL, 150 μg/mL, 200 μg/mL, 250 μg/mL, 500 μgL/mL, 1000 μg/mL) for 48 hours in dark, respectively. The OD values of HL60 cells at different concentrations of nanoparticles were normalized by the OD values of control group (the final concentration of nanoparticles was 0 μg/mL). The relative survival rates of HL60 cells are shown in Figure 7.

As can be seen from Figure 7, with the increasing concentration of nanoparticles solution, the viability of HL60 cells decreased gradually. At a concentration of 1000 μg/mL, the three survival rates were 77%, 73%, 65.3%, respectively. In comparison, when the concentration reduced the range of 0~250 μg/mL, the survival rates of HL60 cells were all above 90%. In this case, the TiO_2 nanoparticles and Fe/TiO_2 nanocomposites could be considered as basically nontoxic materials for cancer cells in the dark, which is in agreement with the suggestions reported in references [27, 28] that TiO_2 is nontoxic for animals.

3.4. Influence of Nanocomposites-Based PDT on the Viability of HL60 Cells. The HL60 cells were inoculated into two 96-well plates marked with A or B. The cell suspensions of A plate were exposed to light after incubating for 24 hours and then preincubated for another 24 hours in the dark. The HL60 cells in plate B were incubated for 48 hours in the incubator without light treatment. The final concentration of nanoparticles TiO_2 nanoparticles or Fe/TiO_2 nanocomposites was 200 μg/mL and each experiment was repeated three times in order to reduce the error. The OD values of experimental groups were then measured by DG5031 ELISA reader, as shown in Table 1.

These measured OD values of cells after light irradiation were normalized by the OD values of cells without light treatment. The relative survival of HL60 and PDT efficiency under different nanoparticles were calculated by the following equations: relative viability = OD_{Light}/OD_{Dark}, and PDT efficiency = 1−relative viability. The results are presented in Figure 8.

According to the measurements shown in Table 1, the OD values of HL60 cells exposed to light are significantly lower than that of the control group without light treatment, for both in the absence and in the presence of nanoparticles. Illumination causes a decline survival rate of tumor cells without TiO_2 nanocomposites which is mainly due to the near-ultraviolet light (403 nm) which itself has a certain degree of killing effect on tumor cells. PDT is designed to "selectively kill tumor cells while not harming normal cells as possible." If light irradiation have a greater killing effect on tumor cell in the absence of photosensitive drugs, it will also inevitably lead to a greater damage to normal cells. Therefore, more attention should be paid to light elements of PDT, to minimize light damage on normal cells. Our previous experiments have demonstrated that the light density of 5 mW/cm^2 and the light irradiation dose of 18 J/cm^2 are the best inactivation parameters of tumor HL60 cells-based photodynamic therapy, which are

Table 1: The influence of light irradiation on OD values of HL60 cells with different nanoparticles. Data and the points are presented as the means ± S.D from tree independent measurements. Statistical analysis was then performed and showed that the differences to be significant ($*P < 0.05$).

	Control		TiO_2		Fe/TiO_2 (2%)		Fe/TiO_2 (5%)	
Light treamernt	1.073	1.092 ±0.031	0.946	0.957 ±0.032	0.937	0.916 ±0.021	0.875	0.881 ±0.006
	1.136		0.921		0.881		0.889	
	1.067		1.004		0.930		0.879	
Without light treamernt	0.440	0.869 ±0.007	0.283	0.283 ±0.015	0.291	0.168 ±0.041	0.231	0.154 ±0.011
	0.434		0.301		0.287		0.254	
	0.452		0.265		0.202		0.256	

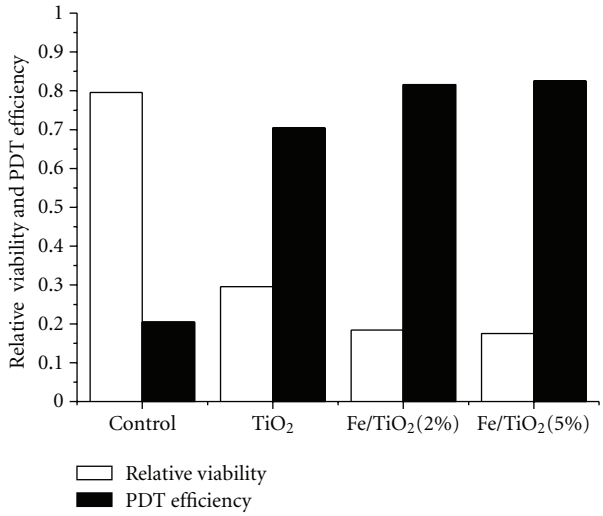

Figure 8: The relative viability of HL60 cells and PDT efficiency of different nanopariticles.

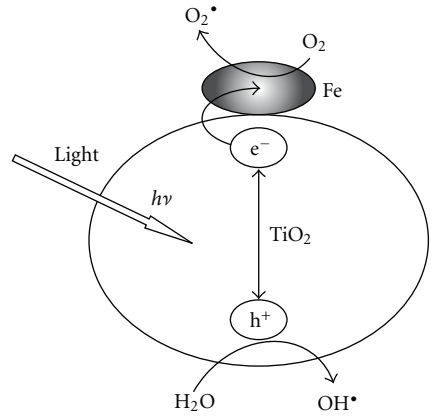

Scheme 1: The possible mechanism of ROS production by Fe-doped TiO_2 nanocomposites under light irradiation.

consistent with the literature reports [29, 30]. Therefore, a more effective approach to solve the problem is to enhance the visible light absorption of TiO_2. Furthermore, the OD values of HL60 cells exposed to light with nanoparticles are significantly lower than these without nanoparticles, which is in agreement with our previous result that nanoparticles have a certain degree of inhibition/toxicity on the growth of cells.

As shown in Figure 8, the relative survival rate of HL60 cells in the presence of nanoparticles is significantly lower than that without nanoparticles. It means that PDT efficiency of HL60 cells with nanoparticles is higher than that of HL60 cells without nanoparticles. In addition, Fe/TiO_2 nanocomposites present much higher efficiency in photokilling HL60 cancer cells than TiO_2 nanoparticles. These results reveal that the modification of Fe on the surface of TiO_2 nanoparticles can greatly enhance the photocatalytic inactivation effect of TiO_2 on HL60 cells. Additionally, Fe/TiO_2 (5%) group displays a little higher inactivation efficiency compared with Fe/TiO_2 (2%) group, when 200 μg/mL Fe/TiO_2 (5%) nanocomposites were added, the inactivation efficiency of HL60 cells can up to 82.5% after a 60-minute irradiation. Although a higher concentration of Fe/TiO_2 nanocomposites or TiO_2 nanoparticles could achieve a higher-photocatalytic killing effect, but it is not preferable to use a very high concentration of photocatalyst for practical consideration as it might block the blood vessels. On the other hand, at high dopant concentrations, due to the decrease of the distance between trapping sites, the recombination rate of the photoinduced electrons and holes increases, resulting in lower photocatalytic activity. Therefore, the doping concentration of Fe should not be too high.

It has been demonstrated that the cell damage mechanism based on ligh-excited Fe/TiO_2 nanocomposites is accomplished through a series of chain reactions by means of reactive oxygen species- (ROS-) induced cell death [31–33].

The generation mechanism of reactive oxygen species (ROS) on Fe-doped TiO_2 nanocomposites under UV irradiation is displayed in Scheme 1. When illuminated by ultraviolet light, photoinduced electrons and holes could be created, which can transfer to the surface of Fe nanoparticles and reduce the dissolved O_2 to produce the superoxide anion

$O^{-\bullet}$. At the same time, the photogenerated holes on the TiO_2 surface can further react with water to generate powerful hydroxyl radicals ($OH^\bullet$) and other oxidative radicals ($HO_2^\bullet$), which are capable of destroying the membrane and component of tumor cells. The recombination rate of the photoproduced electrons and holes can be effectively inhibited by the above process, so the photocatalytic activity of TiO_2 nanoparticles is significantly enhanced by the modification of Fe. Additionally, the enhanced photocatalytic activity of Fe-doped TiO_2 nanocomposites can also be explained by a new energy level produced in the bandgap of TiO_2 due to the dispersion of Fe nanoparticles, as suggested in the literature [30–37]. Regardless of complexity, it is apparent that there are several key photosensitive that have been involved which could be also explained as follows:

$$\begin{aligned} TiO_2 + h\upsilon &\longrightarrow h^+ + e^- \\ H_2O + h^+ &\longrightarrow OH^\bullet + H^+ \\ O_2 + e^- &\longrightarrow O_2^\bullet \longrightarrow HO_2^\bullet \\ 2HO_2^\bullet &\longrightarrow O_2 + H_2O_2 \\ H_2O_2 + O_2^\bullet &\longrightarrow OH^\bullet + OH^- + O_2 \end{aligned} \quad (2)$$

4. Conclusion

In this paper, the prepared Fe/TiO_2 characterized by X-ray diffraction (XRD), transmission electron microscope (TEM), X-ray photoelectron spectroscopy (XPS), and UV-Vis adsorption spectra, respectively, was successfully applied as a photosensitizer-based photodynamic therapy to kill human HL60 cancer cells *in vitro*. The experimental results show that the absorption of TiO_2 nanoparticles in the visible light region could be enhanced effectively by the method of Fe doping, and both pure TiO_2 and Fe/TiO_2 nanocomposites at high concentrations can have a significant inhibition/toxicity on the growth of HL60 cells. It is also found that the photocatalytic inactivation effect on HL60 cells with nanoparticles is obviously higher than that without nanoparticles under the same conditions. Furthermore, Fe/TiO_2 nanocomposites presented much higher PDT efficiency in photokilling HL60 cancer cells than TiO_2 nanoparticles. These indicate that the photocatalytic inactivation effects of TiO_2 on HL60 cells could be greatly improved by the modification of Fe on the surface of TiO_2 nanoparticles. The PDT efficiency of Fe/TiO_2 (5%) nanocomposites on HL60 cells can reach 82.5% at a concentration of 200 μg/mL after a 60-minute light treatment. The high photocatalytic inactivation effects of Fe/TiO_2 nanocomposites on human HL60 cancer cells suggests that it may be an important potential photosensitizer-based photodynamic therapy for cancer treatment [38–40].

Acknowledgments

This work has been financially supported by National Natural Science Foundation of China (61072029), Natural Science Foundation of Guangdong Province (10151063101000025), and Science and Technology Planning Project of Guangzhou city (2010Y1-C111).

References

[1] J. C. Kennedy, R. H. Pottier, and D. C. Pross, "Photodynamic therapy with endogenous protoporphyrin. IX: basic principles and present clinical experience," *Journal of Photochemistry and Photobiology B*, vol. 6, no. 1-2, pp. 143–148, 1990.

[2] A. Lesar, J. Ferguson, and H. Moseley, "An investigation of the fluorescence induced by topical application of 5-aminolaevulinic acid and methyl aminolaevulinate at different body sites on normal human skin," *Photodiagnosis and Photodynamic Therapy*, vol. 8, no. 1, pp. 20–28, 2011.

[3] D. Grebeňová, H. Cajthamlová, J. Bartošová et al., "Selective destruction of leukaemic cells by photo-activation of 5-aminolaevulinic acid-induced protoporphyrin-IX," *Journal of Photochemistry and Photobiology B*, vol. 47, no. 1, pp. 74–81, 1998.

[4] H. S. de Bruijn, W. Sluiter, A. van der Ploeg-van den Heuvel, H. J. C. M. Sterenborg, and D. J. Robinson, "Evidence for a bystander role of neutrophils in the response to systemic 5-aminolevulinic acid-based photodynamic therapy," *Photodermatology Photoimmunology and Photomedicine*, vol. 22, no. 5, pp. 238–246, 2006.

[5] Y. Kubota, T. Shuin, C. Kawasaki et al., "Photokilling of T-24 human bladder cancer cells with titanium dioxide," *British Journal of Cancer*, vol. 70, no. 6, pp. 1107–1111, 1994.

[6] P. Edyta, E. Carsten, O. S. Mathias et al., "Nanodrug applications in photodynamic therapy," *Photodiagnosis and Photodynamic Therapy*, vol. 8, no. 1, pp. 14–29, 2011.

[7] M. Zhou, J. Yu, and B. Cheng, "Effects of Fe-doping on the photocatalytic activity of mesoporous TiO_2 powders prepared by an ultrasonic method," *Journal of Hazardous Materials*, vol. 137, no. 3, pp. 1838–1847, 2006.

[8] P. Juzenas, W. Chen, Y. P. Sun et al., "Quantum dots and nanoparticles for photodynamic and radiation therapies of cancer," *Advanced Drug Delivery Reviews*, vol. 60, no. 15, pp. 1600–1614, 2008.

[9] H. Sakai, R. Baba, K. Hashimoto, Y .Kubota, and A. Fujishima, "Selective killing of a single cancerous cell T24 with TiO_2 semiconducting microelectrode under irradiation," *Chemistry Letters*, vol. 24, no. 3, pp. 185–186, 1995.

[10] J. Gamage and Z. Zhang, "Applications of photocatalytic disinfection," *International Journal of Photoenergy*, vol. 2010, Article ID 764870, 11 pages, 2010.

[11] J. A. Byrne, P. A. Fernandez-Ibañez, P. S. M. Dunlop, D. M. A. Alrousan, and J. W.J. Hamilton, "Photocatalytic enhancement for solar disinfection of water: a review," *International Journal of Photoenergy*, vol. 2011, Article ID 798051, 12 pages, 2011.

[12] N. Lagopati, P. V. Kitsiou, A. I. Kontos et al., "Photo-induced treatment of breast epithelial cancer cells using nanostructured titanium dioxide solution," *Journal of Photochemistry and Photobiology A*, vol. 214, no. 2-3, pp. 215–223, 2010.

[13] Y. Xiong, X. Fei, J. Xiong, and Z. Zhang, "Study on preparation of visible light-activated nitrogen-doped TiO_2 and its photodesdrucing effect on Leukemic HL60 cells in vitro," *Rare Metal Materials and Engineering*, vol. 35, no. 11, pp. 1735–1739, 2006.

[14] L. Tessy, O. Em, A. Mayra et al., "Study of the stabilization of zinc phthalocyanine in sol-gel TiO_2 for photodynamic therapy applications," *Nanomedicine*, vol. 6, no. 6, pp. 777–785, 2010.

[15] L. Chen, J.-W. Xiong, G.-X. Liu, and Z.-X. Zhang, "An experimental study on effects of nanoparticle $TiO_{2-x}N_x$ on inactivation of leukemic HL60 cells in vitro based on ALA-PDT," *Journal of Optoelectronics Laser*, vol. 18, no. 10, pp. 1265–1268, 2007.

[16] A. Di Paola, S. Ikeda, G. Marcì, B. Ohtani, and L. Palmisano, "Transition metal doped TiO_2: physical properties and photocatalytic behaviour," *International Journal of Photoenergy*, vol. 3, no. 4, pp. 171–176, 2001.

[17] M. Jakob, H. Levanon, and P. V. Kamat, "Charge distribution between UV-irradiated TiO_2 and gold nanoparticles: determination of shift in the Fermi level," *Nano Letters*, vol. 3, no. 3, pp. 353–358, 2003.

[18] N. Serpone, A. Salinaro, S. Horikoshi, and H. Hidaka, "Beneficial effects of photo-inactive titanium dioxide specimens on plasmid DNA, human cells and yeast cells exposed to UVA/UVB simulated sunlight," *Journal of Photochemistry and Photobiology A*, vol. 179, no. 1-2, pp. 200–212, 2006.

[19] J. Yu, Q. Xiang, and M. Zhou, "Preparation, characterization and visible-light-driven photocatalytic activity of Fe-doped titania nanorods and first-principles study for electronic structures," *Applied Catalysis B*, vol. 90, no. 3-4, pp. 595–602, 2009.

[20] L. Liu, P. Miao, Y. Xu, Z. Tian, Z. Zou, and G. Li, "Study of Pt/TiO_2 nanocomposite for cancer-cell treatment," *Journal of Photochemistry and Photobiology B*, vol. 98, no. 3, pp. 207–210, 2010.

[21] H. Li, Z. Bian, J. Zhu, Y. Huo, H. Li, and Y. Lu, "Mesoporous Au/TiO_2 nanocomposites with enhanced photocatalytic activity," *Journal of the American Chemical Society*, vol. 129, no. 15, pp. 4538–4539, 2007.

[22] C. Karunakaran, G. Abiramasundari, P. Gomathisankar, G. Manikandan, and V. Anandi, "Cu-doped TiO_2 nanoparticles for photocatalytic disinfection of bacteria under visible light," *Journal of Colloid and Interface Science*, vol. 352, no. 1, pp. 68–74, 2010.

[23] Y.-S. Li, F.-L. Jiang, Q. Xiao et al., "Enhanced photocatalytic activities of TiO_2 nanocomposites doped with water-soluble mercapto-capped CdTe quantum dots," *Applied Catalysis B*, vol. 101, no. 1-2, pp. 118–129, 2010.

[24] J. W. Xiong, H. XIAO, L. Chen, J. M. Wu, and Z. X. Zhang, "Research on different detection conditions between MTT and CCK-8," *Acta Laser Biology Sinica*, vol. 16, no. 5, pp. 526–531, 2007.

[25] C. Lettmann, K. Hildenbrand, H. Kisch, W. Macyk, and W. F. Maier, "Visible light photodegradation of 4-chlorophenol with a coke-containing titanium dioxide photocatalyst," *Applied Catalysis B*, vol. 32, no. 4, pp. 215–227, 2001.

[26] Y. Cong, J. Zhang, F. Chen, M. Anpo, and D. He, "Preparation, photocatalytic activity, and mechanism of Nano-TiO_2 Co doped with nitrogen and Iron (III)," *The Journal of Physical Chemistry C*, vol. 111, no. 28, pp. 10618–10623, 2007.

[27] A. L. Linsebigler, G. Lu, and J. T. Yates, "Photocatalysis on TiO_2 surfaces: principles, mechanisms, and selected results," *Chemical Reviews*, vol. 95, no. 3, pp. 735–758, 1995.

[28] W. G. Wamer, J. J. Yin, and R. R. Wei, "Oxidative damage to nucleic acids photosensitized by titanium dioxide," *Free Radical Biology and Medicine*, vol. 23, no. 6, pp. 851–858, 1997.

[29] Z. X. Zhang, S. J. Zhang, B. Q. Zhang, and M. L. Chen, "Leukemic cells killed by photodynamic therapy with 5 aminolevulinic acid: an experimental study," *Chinese Journal of Laser Medicine & Surgery*, vol. 14, no. 4, pp. 249–252, 2005.

[30] H. Xiao, J. W. Xiong, J. M. Wu, and Z. X. Zhang, "Research of parameters on ALA-PDT destruction of leukaemie cell," *Acta Laser Biology Sinica*, vol. 13, no. 5, pp. 353–357, 2004.

[31] A. Kathiravan and R. Renganathan, "Photoinduced interactions between colloidal TiO_2 nanoparticles and calf thymus-DNA," *Free Radical Biology & Medicine*, vol. 28, no. 7, pp. 1374–1378, 2009.

[32] J. Xu, Y. Sun, J. Huang et al., "Photokilling cancer cells using highly cell-specific antibody-TiO_2 bioconjugates and electroporation," *Bioelectrochemistry*, vol. 71, no. 2, pp. 217–222, 2007.

[33] F. R. James, J. D. Simon, J. F. D. Nicholas, and N. J. Awadhesh, "Hydroxyl radicals (radical dotOH) are associated with titanium dioxide (TiO_2) nanoparticle-induced cytotoxicity and oxidative DNA damage in fish cells," *Mutation Research*, vol. 640, no. 1-2, pp. 113–122, 2008.

[34] J. Xu, Y. Sun, Y. Zhao, J. Huang, C. Chen, and Z. Jiang, "Photocatalytic inactivation effect of gold-doped TiO_2 (Au/TiO_2) nanocomposites on human colon carcinoma LoVo cells," *International Journal of Photoenergy*, vol. 2007, Article ID 97308, 7 pages, 2007.

[35] T. G. Bajnóczi, N. Balázs, K. Mogyorósi et al., "The influence of the local structure of Fe(III) on the photocatalytic activity of doped TiO_2 photocatalysts—an EXAFS, XPS and Mössbauer spectroscopic study," *Applied Catalysis B*, vol. 103, no. 1-2, pp. 232–239, 2011.

[36] Q. Li, C. Zhang, and J. Li, "Photocatalytic and microwave absorbing properties of polypyrrole/Fe-doped TiO_2 composite by in situ polymerization method," *Journal of Alloys and Compounds*, vol. 509, no. 5, pp. 1953–1957, 2011.

[37] H. Fu, G. Shang, S. Yang, and T. Xu, "Mechanistic study of visible-light-induced photodegradation of 4-chlorophenol by $TiO_{2-x}N_x$ ($0.021 < x < 0.049$) with low nitrogen concentration," *International Journal of Photoenergy*, vol. 2012, Article ID 759306, 9 pages, 2012.

[38] K. Naeem and F. Ouyang, "Fe^{+3}-doped TiO_2 nanoparticles and its photocatalytic activity under UV light," *Physica B*, vol. 405, no. 1, pp. 221–226, 2010.

[39] W. H. Suh, K. S. Suslick, G. D. Stucky, and Y. H. Suh, "Nanotechnology, nanotoxicology, and neuroscience," *Progress in Neurobiology*, vol. 87, no. 3, pp. 133–170, 2009.

[40] Y. Yalçin, M. Kiliç, and Z. Çinar, "Fe^{+3}-doped TiO_2: a combined experimental and computational approach to the evaluation of visible light activity," *Applied Catalysis B*, vol. 99, no. 3-4, pp. 469–477, 2010.